Gadolinium oxide for molecular and cellular MRI: A cautionary tale

S. S. Williams[1,2], T. L. Lobo[3], and E. M. Shapiro[1,3]
[1]Department of Biomedical Engineering, Yale University, New Haven, CT, United States, [2]Xavier University of Louisiana, New Orleans, LA, United States,
[3]Department of Diagnostic Radiology, Yale University School of Medicine, New Haven, CT, United States

INTRODUCTION: Superparamagnetic iron oxide particles generate dark contrast on T_2 or T_2* weighted MRI. A perceived drawback to their usage for cell tracking is that dark contrast in MRI can be generated by other biological and physical phenomena. To avoid these ambiguities, a potential mechanism for producing bright contrast for labeled cells in MRI is to use high r_1 relaxivity contrast agents. Cells would then appear bright on T_1 weighted MRI. Recently, Gd_2O_3 has been investigated for targeted MRI (1). Depending on size, Gd_2O_3 can have an r_1 of ~ 10 $mM^{-1}s^{-1}$ (1). Thus, Gd_2O_3 appears to be a good candidate for an MRI-based cell tracking agent which would enable bright contrast on T_1 weighted MRI. But it's not that straightforward.

In this work, we fabricated and characterized polymer encapsulated Gd_2O_3 nanocrystals. We then assayed them to determine whether they would be suitable for MRI-based cell tracking, both in terms of MRI properties, as well as safety. It was found that polymer encapsulated Gd_2O_3 nanocrystals have sufficient r_1 relaxivity to enable MRI-based cell tracking, however, similar to inorganic manganese based materials (2), Gd_2O_3 nanocrystals rapidly dissolve in acidic conditions which mimic the endosomal/lysosomal environment within the cells to form Gd^{3+} ions. As such, this is a cautionary tale in the use of Gd_2O_3 nanocrystals for MRI-based cell tracking.

MATERIALS AND METHODS: Gd_2O_3 nanocrystals were synthesized by thermal decomposition of gadolinium (III) acetylacetonate. PLGA encapsulated Gd_2O_3 nanoparticles were formed using a single emulsion technique. Weight percents of Gd_2O_3 to PLGA during fabrication were 0, 10, 30 or 50%. Oleic acid was used as an excipient to enhance encapsulation. Gd_2O_3 nanocrystals and intact PLGA encapsulated particles were characterized by powder x-ray diffraction (XRD), transmission electron microscopy (TEM) and scanning electron microscopy (SEM). Total Gd_2O_3 content of the particles was measured by inductively coupled plasma optical emission spectroscopy (ICP). r_1 molar relaxivity of Gd_2O_3 embedded particles was measured at 4.0 Tesla.

Dissolution studies were performed on both naked Gd_2O_3 nanocrystals as well as Gd_2O_3 doped PLGA nanoparticles, in both PBS pH 7.4 and 20 mM citrate buffer, pH 5.0, mimicking both cytosolic and lysosomal environments, respectively. To evaluate the ability of the NPs to label cells, either 0, 50, 100 or 200 µl of 10 mg/ml Gd_2O_3 50 wt% NP in 10 ml media was added to confluent culture dishes of cells (~ 5 million cells) and allowed to incubate for 24 hours. Cells were then washed with PBS to remove free particles, trypsinized, and centrifuged to form cell pellets. Cells were also tested for viability. Cell pellets then underwent T_1 and T_2 mapping at 4.0 Tesla. Bright field photomicrographs of labeled cells were also acquired. After MRI, ICP was again used to determine amount of Gd_2O_3 internalized into cells.

RESULTS and DISCUSSION: TEM revealed that Gd_2O_3 nanocrystals were 3-5 nm. XRD identified the crystal structure of the Gd_2O_3 with broad lines confirming the extreme small size of the nanocrystals. Figure 1A,B show SEM of PLGA encapsulated Gd_2O_3 nanoparticles for formulations containing 0 and 50 wt% Gd_2O_3. Smooth, spherical nanoparticles with low polydispersity were obtained with sizes of 182.2 +/- 50.6, 131.4 +/- 30.4 and 142.0 +/- 38.8 nm, for 0, 30 and 50 wt %, respectively. Encapsulation efficiencies as high as ~ 60% and total Gd content of ~ 20% wt% were obtained for different formulations. The r_1 molar relaxivity of PLGA encapsulated Gd_2O_3 nanoparticles was measured to be 1.9 $mM^{-1}sec^{-1}$, larger than previously reported manganese based nanoparticles for molecular and cellular MRI (3-5).

Dissolution of Gd_2O_3 cores in citrate to form Gd^{3+} occurred rapidly, with nearly half dissolving within 18 minutes, while there was negligible dissolution in PBS (Figure 2A). In addition to dissolution of Gd_2O_3 cores, evolution of Gd^{3+} from PLGA encapsulated Gd_2O_3 was investigated over the course of 2 days, again in PBS and citrate buffer. While dissolution of Gd_2O_3 cores in PBS was negligible over 48 hours in PBS, Figure 2B shows that ~90% of the Gd_2O_3 cores was dissolved by 1 hour and 99% at 24 hours. These rates of metallic core dissolution, both as naked cores and as polymer encapsulated cores, are much faster than we have measured for both iron oxide and manganese oxide, and are likely due to the extremely small size of the Gd_2O_3 synthesized in this work.

Lastly, cells were labeled with different amounts of Gd_2O_3 particles for 24 hours. Viability at 24 hours via trypan blue staining was >95% for all samples. Cell pellets were subjected to T_1 and T_2 mapping by MRI. Figure 3A,B show the T_1 and T_2 data from the different cell treatments. As can be seen, cells labeled with more Gd_2O_3 particles have shorter T_1 and T_2. However, for each treatment group, the change in R_2, which is linear with respect to concentration of agent, greatly exceeded the change in R_1. This means that internalized Gd_2O_3 NPs are more efficient T_2 agents than T_1 agents. This is not surprising given the body of work describing the quenching of Gd^{3+} relaxivity in intracellular environment (6), and the likely formation of Gd^{3+} inside cells following internalization.

CONCLUSION: Polymer encapsulated Gd_2O_3 nanocrystals have sufficient r_1 relaxivity to enable MRI-based cell tracking and can be internalized into phagocytic cells, resulting in T_1 and T_2 enhancement. However, Gd_2O_3 nanocrystals rapidly dissolve in acidic conditions which mimic the endosomal/lysosomal environment within the cells, evolving Gd^{3+}. Despite high cellular viability at 24 hours, this has severe implications not only for MRI-based cell tracking, but also for targeted Gd_2O_3 nanocrystals, as following systemic administration, some particles could be phagocytosed in the RES and could potentially form Gd^{3+}. While this might not necessarily kill the cells, there is little doubt as to the contribution of Gd^{3+} to NSF. As such, caution is urged for the use of Gd based particles for molecular and cellular MRI.

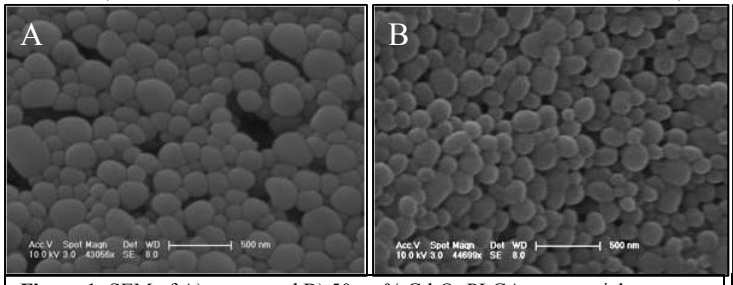

Figure 1: SEM of A) empty and B) 50 wt % Gd_2O_3 PLGA nanoparticles.

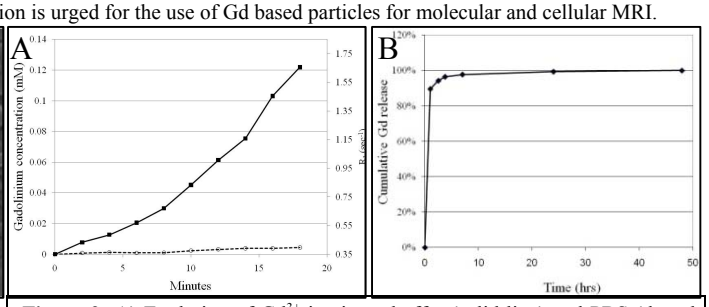

Figure 2: A) Evolution of Gd^{3+} in citrate buffer (solid line) and PBS (dotted line) from Gd_2O_3 cores. B) Gd^{3+} evolution from Gd_2O_3 doped PLGA nanoparticles in citrate buffer.

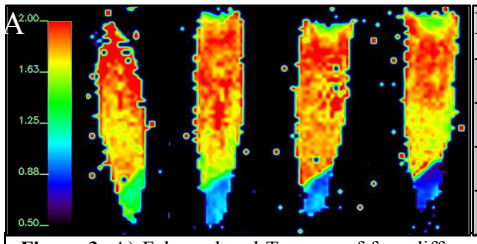

B

Sample	T_1 (sec)	R_1 (sec^{-1})	ΔR_1	T_2 (sec)	R_2 (sec^{-1})	ΔR_2	[Gd] (pg/cell)
0	1.24	0.81	—	0.146	6.85	—	0
50	1.04	0.96	19%	0.101	9.90	45%	2.53
100	0.95	1.05	31%	0.087	11.5	68%	7.14
200	0.82	1.22	51%	0.67	14.9	118%	14.6

Figure 3: A) False colored T_1 maps of four different cell samples loaded with 0, 50, 100 or 200 µl of labeling solution for 24 hours, from left to right. Cell pellets are displayed in green or blue. Scale bar is T_1 in seconds. B) Table showing T_1,R_1 and T_2,R_2 for cell pellets, coordinated with amount of internalized Gd.

References:
1. J. Y. Park *et al.*, *Acs Nano* **3**, 3663 (2009). **2.** E. M. Shapiro, A. P. Koretsky, *Magn Reson. Med.* **60**, 265 (2008). **3.** H. B. Na *et al.*, *Angew. Chem. Int. Ed Engl.* **46**, 5397 (2007). **4.** J. Shin *et al.*, *Angew. Chem. Int. Ed Engl.* **48**, 321 (2009). **5.** C. C. Huang *et al. Biomaterials* **31**, 4073 (2010). **6.** C. S. Geninatti *et al.*, *J. Biol. Inorg. Chem.* **10**, 78 (2005).

NIH grants P30 NS052519 and DP2 OD004362